Variable high-gain disturbance observer design with online adaption of observer gains embedded in numerical integration

Yan Liu*, Dirk Söffker

Chair of Dynamics and Control, University of Duisburg-Essen, Lotharstr. 1-21, 47057, Duisburg, Germany

Abstract

In this paper, a variable gain design approach for the high-gain disturbance observer, called Proportional-Integral-Observer (PI-Observer), is proposed to solve the problem of choosing suitable observer gains. The high-gain PI-Observer is successfully applied to estimate unknown inputs of systems together with the system states. It is known that reasonable estimations of unknown inputs can only be derived using high observer gains. On the other hand, extremely large gains will cause serious problems with respect to measurements noise and unmodeled dynamics. According to the analysis of the estimation quality regarding to the factors which influence the estimation results, the optimal level of observer gains is changing during the estimation, an online adaption for the observer gains is therefore developed. The designed PI-Observer, called Advanced PI-Observer (API-Observer), will use changing observer gains from the adaption algorithm, which is proved to give stable estimation error dynamics. Simulation results from an elastic beam example are shown to illustrate the implementation of the API-Observer.

Key words: High-gain observer; Disturbance observer; Variable gain observer

1. Introduction and motivation

To mitigate large overshooting behavior and the correspondent high input control signals and to reduce influence from measurement noise and unmodeled dynamics, high observer

*Corresponding author. Tel.: 0049 203 3791577; fax: 0049 203 379 3027

Email addresses: yan.liu@uni-due.de (Yan Liu), soeffker@uni-due.de (Dirk Söffker)

gains for estimating weakly observable eigenmotions (eigenmotions with large correspondent condition number in the observability matrix) are usually prevented. In spite of this, special properties and application fields of high-gain Proportional-Integral-Observer (PI-Observer) are later found very valuable. The observer technique using additional integral part and corresponding extended states was already introduced by Wojciechowski [10] and then developed by different authors [2, 7] with different design goals. The goal of the high gain PI-Observer is to estimate unknown inputs to the system by using high observer gains. However, the basic problem using high observer gains the conflict between the time behavior/quality of estimation and the sensitivity to measurement noise/unmodeled dynamics still has to be accounted during the development/application of high-gain PI-Observer. This motivates the work in this paper, namely to choose or keep suitable gains for an high-gain observer design. In the paper, an approach is proposed to provide a convenient online adaption algorithm to keep the gains of the PI-Observer always at a rational level regarding the current influence from different aspects.

The underlying task improving the observer gain design is explored by other researchers in [1, 3]. Most of them recommend solutions for variable observer gains between two fixed observer gains (usually one high gain and one low gain) according to distinguished switching conditions. Of course using two gains to be switched is under the consideration of the clarity of the programming and the simplification of the structure. However, the problem choosing suitable observer gains for the high gain PI-Observer can only be roughly solved with approaches using two fixed observer gains, because the level of the high and low gains is difficult to be determined to match every case of the changing unknown inputs. For example, in [3] the observer gains are switched once regarding the transient time, but for high gain PI-Observer design the dynamics of the unknown inputs (also of modeling disturbances) may strongly change along the time and several switches with different transient time intervals may be necessary. In [1] the observer gains are also switched regarding to pre-defined transient time, but more generally the switch is not limited as only once. However, both the two given observer gains have to be suitably chosen in advance. That means the high observer gains have to be determined based on assumed situations which can not match every requirement during the whole working time and this approach is not a suitable one to solve the mentioned problem to choose suitable gains for the high gain PI-Observer.

In this contribution, an optimal level of the PI-Observer gains for general use is defined and analyzed. A solution strategy based on a bank of observers is proposed to get a high gain PI-Observer design that can adapt its observer gains to the current situation. In this concept, two parallel running PI-Observers are simulated together with the main PI-Observer whose estimation results will be taken. One is working with observer gains larger than the current main PI-Observer, the other with observer gains smaller than the current main PI-Observer. The value of suitable chosen cost functions will be compared to get the current rational level of the observer gain. The whole adaption algorithm is embedded in the numerical algorithm of the observer. A novel feature of the algorithm includes the adaption process into the numerically defined step-size control of the numerical integration procedure used to realize observers functionality in general. The proposed high gain PI-Observer design with online adaption for observer gains and a bank of PI-Observers is called Advanced PI-Observer (API-Observer).

The contributions of the paper are:

- analysis of the optimal level of the observer gains for a PI-Observer,
- embedded adaption algorithm in the numerical integration procedure,
- proof of the stability of estimation error dynamics while using the API-Observer, and
- a practical example estimating contact force of a vibrating elastic beam.

The paper is organized as follows: In the second section, high gain PI-Observer design is briefly introduced. The adaption algorithm for the high gain design and the related theoretical background are discussed in the third section. Simulation results in the fourth section show the adaption process of the observer gains in application. Summary and conclusions are given in the last section.

2. Problem statement

For a class of systems described by

$$\dot{\boldsymbol{x}}(t) = \boldsymbol{A}\boldsymbol{x}(t) + \boldsymbol{B}\boldsymbol{u}(t) + \boldsymbol{N}\boldsymbol{d}(\boldsymbol{x}, t) + \boldsymbol{E}\boldsymbol{g}(t), \tag{1}$$

$$\boldsymbol{y}(t) = \boldsymbol{C}\boldsymbol{x}(t) + \boldsymbol{h}(t), \tag{2}$$

with the state vector $\boldsymbol{x}(t) \in \mathbb{R}^n$, the input vector $\boldsymbol{u}(t) \in \mathbb{R}^l$, the measurement vector $\boldsymbol{y}(t) \in \mathbb{R}^m$, the time variant and unknown inputs $\boldsymbol{d}(\boldsymbol{x}, t) \in \mathbb{R}^r$, the measurement noise $\boldsymbol{h}(t) \in \mathbb{R}^m$, and the unmodeled dynamics $\boldsymbol{E}\boldsymbol{g}(t)$ with $\boldsymbol{g}(t) \in \mathbb{R}^p$ and $\boldsymbol{E} \in \mathbb{R}^{n\times p}$. Here, the information about the dynamics of $\boldsymbol{d}(\boldsymbol{x}, t)$ is assumed as not available. Only the matrix $\boldsymbol{N}$ (related to the system description) denoting the position of the unknown inputs acting to the system is assumed as known. The aim is, with the given information of the system model, the matrices $\boldsymbol{A} \in \mathbb{R}^{n\times n}$, $\boldsymbol{B} \in \mathbb{R}^{n\times l}$, $\boldsymbol{C} \in \mathbb{R}^{m\times n}$, and $\boldsymbol{N} \in \mathbb{R}^{n\times r}$, to estimate the dynamical behavior of the system and the dynamics of the unknown inputs. The system matrix $\boldsymbol{A}$ is assumed stable. A high-gain PI-Observer can be designed in this case to get the estimations of the original states $\boldsymbol{x}(t)$ and the unknown inputs $\boldsymbol{d}(\boldsymbol{x}, t)$[4].

2.1. High-gain PI-Observer design

In this part, the general high-gain PI-Observer design developed in [8] for the considered class of systems (1)-(2) will be introduced briefly. The purpose of the approach is the robust estimation of unknown inputs without any assumptions about their dynamics.

2.1.1. Structure of a high-gain PI-Observer

The states $\boldsymbol{x}(t)$ and the unknown inputs $\boldsymbol{d}(\boldsymbol{x}, t)$ in (1) can be estimated by a high-gain observer design

$$\begin{bmatrix} \dot{\hat{\boldsymbol{x}}}(t) \\ \dot{\hat{\boldsymbol{d}}}(t) \end{bmatrix} = \underbrace{\begin{bmatrix} \boldsymbol{A} & \boldsymbol{N} \\ \boldsymbol{0} & \boldsymbol{0} \end{bmatrix}}_{\boldsymbol{A_e}} \begin{bmatrix} \hat{\boldsymbol{x}}(t) \\ \hat{\boldsymbol{d}}(t) \end{bmatrix} + \underbrace{\begin{bmatrix} \boldsymbol{B} \\ \boldsymbol{0} \end{bmatrix}}_{\boldsymbol{B_e}} \boldsymbol{u}(t) + \underbrace{\begin{bmatrix} \boldsymbol{L_1} \\ \boldsymbol{L_2} \end{bmatrix}}_{\boldsymbol{L}} (\boldsymbol{y}(t) - \hat{\boldsymbol{y}}(t)), \tag{3}$$

$$\hat{\boldsymbol{y}}(t) = \underbrace{\begin{bmatrix} \boldsymbol{C} & \boldsymbol{0} \end{bmatrix}}_{\boldsymbol{C_e}} \begin{bmatrix} \hat{\boldsymbol{x}}(t) \\ \hat{\boldsymbol{d}}(t) \end{bmatrix}. \tag{4}$$

The structure and the design of the PI-Observer are similar to the design of Extended Kalman Filters. But the focus here, using the extended integral parts in the observer to estimate the unknown inputs, is different from the Extended Kalman Filter (instead of parameters of a given model here the unmodeled unknown input is used as additional state). To achieve this goal, a requirement for the PI-Observer design has to be fulfilled: the extended system ($\boldsymbol{A_e}$, $\boldsymbol{C_e}$) has to be fully observable, which implies that the condition

$$rank \begin{bmatrix} \lambda I_n - \boldsymbol{A} & -\boldsymbol{N} \\ \boldsymbol{0} & \lambda \boldsymbol{I}_r \\ \boldsymbol{C} & \boldsymbol{0} \end{bmatrix} = n + r \tag{5}$$

for all the eigenvalues λ of A_e has to be fulfilled. This condition includes that the dimension of the unknown input vector $\boldsymbol{d}(t)$ has to be less than or equal to the number of independent measurements, namely $r \leq m$ (Proofs refer to [8, 6]). It gives simultaneously the information that the measurements/the outputs and the states are coupled together to some extent.

Based on Eq. (3) and Eq. (4), considering the estimation errors as $\boldsymbol{e}(t) = \hat{\boldsymbol{x}}(t) - \boldsymbol{x}(t)$ and $\boldsymbol{f_e}(t) = \hat{\boldsymbol{d}}(t) - \boldsymbol{d}(\boldsymbol{x}, t)$, the error dynamics of the extended system becomes

$$\begin{bmatrix} \dot{\boldsymbol{e}}(t) \\ \dot{\boldsymbol{f}}_{\boldsymbol{e}}(t) \end{bmatrix} = \underbrace{\begin{bmatrix} \boldsymbol{A} - \boldsymbol{L}_1\boldsymbol{C} & \boldsymbol{N} \\ -\boldsymbol{L}_2\boldsymbol{C} & \boldsymbol{0} \end{bmatrix}}_{\boldsymbol{A_{e,obs}}} \begin{bmatrix} \boldsymbol{e}(t) \\ \boldsymbol{f_e}(t) \end{bmatrix} - \begin{bmatrix} \boldsymbol{Eg}(t) \\ \dot{\boldsymbol{d}}(\boldsymbol{x}, t) \end{bmatrix} + \underbrace{\begin{bmatrix} \boldsymbol{L_1} \\ \boldsymbol{L_2} \end{bmatrix}}_{\boldsymbol{L}} h(t). \tag{6}$$

For a suitable observer design, the feedback matrix $\boldsymbol{L}$ has to be chosen in such a way that the estimation errors tend to zero ($\boldsymbol{e} \rightarrow \boldsymbol{0}$, $\boldsymbol{f_e} \rightarrow \boldsymbol{0}$). The error dynamics (6) is affected by the term $\dot{\boldsymbol{d}}(\boldsymbol{x}, t)$. In [4, 8], the approximative decoupling $\dot{\boldsymbol{d}}(t)$ to $\boldsymbol{e}(t)$, $\boldsymbol{f_e}(t)$ by applying high gains matrix $\boldsymbol{L}$ is introduced and will be repeated here briefly. The error dynamics (6) for stationary behavior can be described by

$$\boldsymbol{e}(s) = \boldsymbol{G}^{-1}\boldsymbol{N}\boldsymbol{f_e}(s) - \boldsymbol{G}^{-1}\boldsymbol{Eg}(s) + \boldsymbol{G}^{-1}\boldsymbol{L}_1\boldsymbol{h}(s)\ , \tag{7}$$

$$\begin{aligned} \boldsymbol{f_e}(s) = & -[s\boldsymbol{I} + \boldsymbol{L}_2\boldsymbol{C}\boldsymbol{G}^{-1}\boldsymbol{N}]^{-1} s\, \boldsymbol{d}(s) \\ & + [s\boldsymbol{I} + \boldsymbol{L}_2\boldsymbol{C}\boldsymbol{G}^{-1}\boldsymbol{N}]^{-1}\boldsymbol{L}_2\boldsymbol{C}\boldsymbol{G}^{-1}\boldsymbol{Eg}(s) \\ & + [s\boldsymbol{I} + \boldsymbol{L}_2\boldsymbol{C}\boldsymbol{G}^{-1}\boldsymbol{N}]^{-1}\boldsymbol{L}_2(\boldsymbol{I} - \boldsymbol{C}\boldsymbol{G}^{-1}\boldsymbol{L}_1)\boldsymbol{h}(s), \end{aligned} \tag{8}$$

with $\boldsymbol{G} = [s\boldsymbol{I} - (\boldsymbol{A} - \boldsymbol{L}_1\boldsymbol{C})]$. The state estimation error $\boldsymbol{e}(s)$ and the estimation error of unknown inputs $\boldsymbol{f_e}(s)$ are considered separately. The feedback matrices $\boldsymbol{L}_1$ and $\boldsymbol{L}_2$ are required to stabilize the extended system described by the matrix $\boldsymbol{A_{e,obs}}$ and are also required to minimize the influence from the disturbance $\dot{\boldsymbol{d}}(t)$ as unknown inputs to the estimations $\boldsymbol{e}(t)$ and $\boldsymbol{f_e}(t)$. From Eq. (8), it can be seen that to minimize the influence, the transfer function from $s\boldsymbol{d}(s)$ to $\boldsymbol{f_e}(s)$ should satisfy $\left\|[\boldsymbol{I}s + \boldsymbol{L}_2\boldsymbol{C}\boldsymbol{G}^{-1}\boldsymbol{N}]^{-1}\right\|_\infty \leq \gamma, \;\; \gamma \longrightarrow Minimum.$

Assuming without loss of generality a full rank of matrix $\boldsymbol{G}$ and high gains of $\boldsymbol{L}_2$, the values of $\boldsymbol{L}_1$ in $\boldsymbol{G}$ are smaller relative to $\boldsymbol{L}_2$ ($\|\boldsymbol{L}_2\|_F \gg \|\boldsymbol{L}_1\|_F$[1]), so that γ becomes very small. Assuming that the unknown inputs $\|s\,\boldsymbol{d}(s)\|_F$ are bounded, the estimation error $\|\boldsymbol{f_e}(s)\|_F$ can be reduced to an arbitrary small value (but not to zero), if the measurement noise and the unmodeled dynamics are not taken into account.

From the two other parts in Eq. (8), large $\|\boldsymbol{L}_2\|_F$ will increase the influence from measurement noise $h(s)$ and unmodeled dynamics $g(s)$ to the estimation error $\|\boldsymbol{f_e}(s)\|_F$. In [4, 8] detailed proofs and further applications are given.

2.1.2. Design of observer gains

The Linear Quadratic Regulator (LQR) method can be applied to design the high-gain PI-Observer feedback matrices by solving the algebraic matrix Riccati equation. Later on for the optimization of observer gain matrices design this method will be used.

For a stable observer, suitable observer gains can be calculated, if for given positive definite matrices $\boldsymbol{Q}$, $\boldsymbol{R}$ the Riccati equation

$$\boldsymbol{A}_e\boldsymbol{P} + \boldsymbol{P}\boldsymbol{A}_e^T + \boldsymbol{Q} - \boldsymbol{P}\boldsymbol{C}_e^T\boldsymbol{R}^{-1}\boldsymbol{C}_e\boldsymbol{P} \;\; = \;\; \boldsymbol{0} \qquad (9)$$

has a unique positive definite solution matrix $\boldsymbol{P}$. The observer feedback matrix is then calculated with $\boldsymbol{L} = \boldsymbol{P}\boldsymbol{C}_e^T\boldsymbol{R}^{-1}$.

---

[1]The norm $\|\cdot\|_F$ denotes here the Frobenius norm, $\|A\|_F = \sqrt{\sum_{i=1}^{m}\sum_{j=1}^{n} a_{ij}^2} = \sqrt{trace(A^*A)}$ for A in $R^{m\times n}$.

3. Proposed API-Observer design

The purpose of the API-Observer design is to find suitable observer gains to get reasonable/acceptable estimation errors for both the state and the unknown input. The optimization problem of the adaptive scheme for observer gains is formulated in the following and one algorithm for the problem is given next.

3.1. Formulation of the optimization problem

As discussed in section 2.1.1, high observer gains, which are evaluated here by $\|\boldsymbol{L_2}\|_F$, will lead to possibly non-negligible influence from measurement noise and unmodeled dynamics. On the other hand, the ratio between $\|\boldsymbol{L}_2\|_F$ and $\|\boldsymbol{L}_1\|_F$, $\delta = \|\boldsymbol{L}_2\|_F/\|\boldsymbol{L}_1\|_F$, should be large to compensate the effect from the unknown input dynamics. These principle aspects can be seen from the discussion in Eq. (7) and (8).

To illustrate the conflict/the problem clearly and tersely, here without loss of generality the weighting matrices in Eq. (9) are chosen as

$$\boldsymbol{Q} = \begin{bmatrix} \boldsymbol{I}_n & \boldsymbol{0}_{n\times r} \\ \boldsymbol{0}_{r\times n} & q\boldsymbol{I}_r \end{bmatrix}, \quad \boldsymbol{R} = \boldsymbol{I}_m, \tag{10}$$

with only one scalar design parameter $q > 0$.

It can be proven that the parameter q can reflect almost all the important aspects which should be considered. Using the given definitions of the weighting matrices, the solution of the Riccati equation and the observer gain matrix can be calculated by

$$\boldsymbol{P} = \begin{bmatrix} \boldsymbol{P}_{11} & \boldsymbol{P}_{12} \\ \boldsymbol{P}_{12}^T & \boldsymbol{P}_{22} \end{bmatrix}, \tag{11}$$

$$\boldsymbol{L} = \boldsymbol{P}\boldsymbol{C}_e^T = \begin{bmatrix} \boldsymbol{P}_{11}\boldsymbol{C}^T \\ \boldsymbol{P}_{12}^T\boldsymbol{C}^T \end{bmatrix}, \tag{12}$$

$$\boldsymbol{A}\boldsymbol{P}_{11}+\boldsymbol{P}_{11}\boldsymbol{A}^T-\boldsymbol{P}_{11}\boldsymbol{C}^T\boldsymbol{C}\boldsymbol{P}_{11}=-(\boldsymbol{I}_n+\boldsymbol{N}\boldsymbol{P}_{12}^T+\boldsymbol{P}_{12}\boldsymbol{N}^T), \tag{13}$$

$$\boldsymbol{P}_{12}^T\boldsymbol{C}^T\boldsymbol{C}\boldsymbol{P}_{12} = q\boldsymbol{I}_r, \tag{14}$$

$$\boldsymbol{A}\boldsymbol{P}_{12} + \boldsymbol{N}\boldsymbol{P}_{22} = \boldsymbol{P}_{11}\boldsymbol{C}^T\boldsymbol{C}\boldsymbol{P}_{12}. \tag{15}$$

For the design/proof, the relation between the preferred design parameter q, the norm $\|\boldsymbol{L_2}\|_F$ and the ratio δ is considered.

3.1.1. Theoretical analysis of the relation among the design parameter q, the norm $\|\boldsymbol{L_2}\|_F$, and the ratio δ

Theorem 1. *For increasing design parameter q, the ratio δ, and the norm $\|\boldsymbol{L_2}\|_F$ will increase correspondingly.*

Mathematical description:

For two general design parameters q_a and q_b, the corresponding solution matrices $\boldsymbol{P^a}$ and $\boldsymbol{P^b}$ are denoted by

$$\boldsymbol{P^a} = \begin{bmatrix} \boldsymbol{P}^a_{11} & \boldsymbol{P}^a_{12} \\ \boldsymbol{P}^{a\ T}_{12} & \boldsymbol{P}^a_{22} \end{bmatrix} \text{ and } \boldsymbol{P^b} = \begin{bmatrix} \boldsymbol{P}^b_{11} & \boldsymbol{P}^b_{12} \\ \boldsymbol{P}^{b\ T}_{12} & \boldsymbol{P}^b_{22} \end{bmatrix}. \tag{16}$$

Similarly,

$$\boldsymbol{L}^a = \begin{bmatrix} \boldsymbol{L}^a_1 \\ \boldsymbol{L}^a_2 \end{bmatrix} = \begin{bmatrix} \boldsymbol{P}^a_{11}\boldsymbol{C}^T \\ \boldsymbol{P}^{a\ T}_{12}\boldsymbol{C}^T \end{bmatrix} \text{ and } \boldsymbol{L}^b = \begin{bmatrix} \boldsymbol{L}^b_1 \\ \boldsymbol{L}^b_2 \end{bmatrix} = \begin{bmatrix} \boldsymbol{P}^b_{11}\boldsymbol{C}^T \\ \boldsymbol{P}^{b\ T}_{12}\boldsymbol{C}^T \end{bmatrix} \tag{17}$$

are used.

If the parameters fulfill $q_a > q_b > 0$, it follows that

i) $\|\boldsymbol{L}^a_2\|_F > \left\|\boldsymbol{L}^b_2\right\|_F$ *and correspondingly*

ii) $\delta^a = \|\boldsymbol{L}^a_2\|_F / \|\boldsymbol{L}^a_1\|_F > \delta^b = \left\|\boldsymbol{L}^b_2\right\|_F / \left\|\boldsymbol{L}^b_1\right\|_F$.

Proof. i) The matrices $\boldsymbol{P^a}$ and $\boldsymbol{P^b}$ are solution matrices of the Riccati equation (6), satisfying the equation (8), which can be rewritten by

$$\boldsymbol{P}^T_{12}\boldsymbol{C}^T\boldsymbol{C}\boldsymbol{P}_{12} = (\boldsymbol{C}\boldsymbol{P}_{12})^T(\boldsymbol{C}\boldsymbol{P}_{12}) = q\boldsymbol{I}_r. \tag{18}$$

Considering the trace of the matrices in (10), it follows

$$tr((\boldsymbol{C}\boldsymbol{P}_{12})^T(\boldsymbol{C}\boldsymbol{P}_{12})) = tr(\boldsymbol{L_2}\boldsymbol{L_2}^T) = tr(q\boldsymbol{I}_r) = rq, \tag{19}$$

so each expression is described using r. Considering the above obtained results, the norm of the gain matrix can also be expressed to

$$\|\boldsymbol{L_2}\|_F = \left\|\boldsymbol{L_2}^T\right\|_F = \sqrt{tr(\boldsymbol{L_2}\boldsymbol{L_2}^T)} = \sqrt{rq}. \tag{20}$$

With the assumption $q_a > q_b > 0$ and r as constant, it holds

$$\|\boldsymbol{L}_2^a\|_F = \sqrt{rq_a} > \sqrt{rq_b} = \left\|\boldsymbol{L}_2^b\right\|_F. \tag{21}$$

$$\Rightarrow \|\boldsymbol{L}_2^a\|_F > \left\|\boldsymbol{L}_2^b\right\|_F. \tag{22}$$

ii) From (7)

$$\boldsymbol{P}_{11}\boldsymbol{C}^T\boldsymbol{C}\boldsymbol{P}_{11} = \boldsymbol{A}\boldsymbol{P}_{11} + \boldsymbol{P}_{11}\boldsymbol{A}^T + (\boldsymbol{I}_n + \boldsymbol{N}\boldsymbol{P}_{12}^T + \boldsymbol{P}_{12}\boldsymbol{N}^T), \tag{23}$$

it can be obtained

$$\begin{aligned} \|\boldsymbol{L}_1\|_F^2 &= \left\|\boldsymbol{P}_{11}\boldsymbol{C}^T\right\|_F^2 = tr(\boldsymbol{P}_{11}\boldsymbol{C}^T\boldsymbol{C}\boldsymbol{P}_{11}) \\ &= tr(\boldsymbol{A}\boldsymbol{P}_{11} + \boldsymbol{P}_{11}\boldsymbol{A}^T) + n + tr(\boldsymbol{N}\boldsymbol{P}_{12}^T + \boldsymbol{P}_{12}\boldsymbol{N}^T) \\ &= 2tr(\boldsymbol{A}\boldsymbol{P}_{11}) + n + 2tr(\boldsymbol{N}\boldsymbol{P}_{12}^T). \end{aligned} \tag{24}$$

Therefore, it follows

$$\|\boldsymbol{L}_1^a\|_F^2 - \left\|\boldsymbol{L}_1^b\right\|_F^2 = 2tr(\boldsymbol{A}(\boldsymbol{P^a}_{11} - \boldsymbol{P^b}_{11})) + 2tr(\boldsymbol{N}(\boldsymbol{P^a}_{12} - \boldsymbol{P^b}_{12})^T). \tag{25}$$

It is obvious that the matrices $Q_a \geq Q_b$ [2] for $q_a > q_b > 0$. If the algebraic Riccati equation (8) is considered, then it can be obtained that $\boldsymbol{P^a} \geq \boldsymbol{P^b}$, because of the monotonicity of maximal solutions of algebraic Riccati equations [9].

Due to the assumed stability of the matrix A, the extended system matrix A_e is also stable. Considering the condition $\boldsymbol{P^a} \geq \boldsymbol{P^b}$, it holds then

$$(\boldsymbol{P^a} - \boldsymbol{P^b})\boldsymbol{A}_e + (\boldsymbol{P^a} - \boldsymbol{P^b})\boldsymbol{A}_e^T = \tilde{\boldsymbol{H}} = \begin{bmatrix} \tilde{\boldsymbol{H}}_1 & \tilde{\boldsymbol{H}}_2 \\ \tilde{\boldsymbol{H}}_3 & \tilde{\boldsymbol{H}}_4 \end{bmatrix} \geq 0, \tag{26}$$

[2]Note that if the matrices A and $A - B$ are positive semidefinite, it is written here $A \geq 0$ and $A \geq B$ or $B \leq A$ respectively. A and B are assumed to be hermitian matrices.

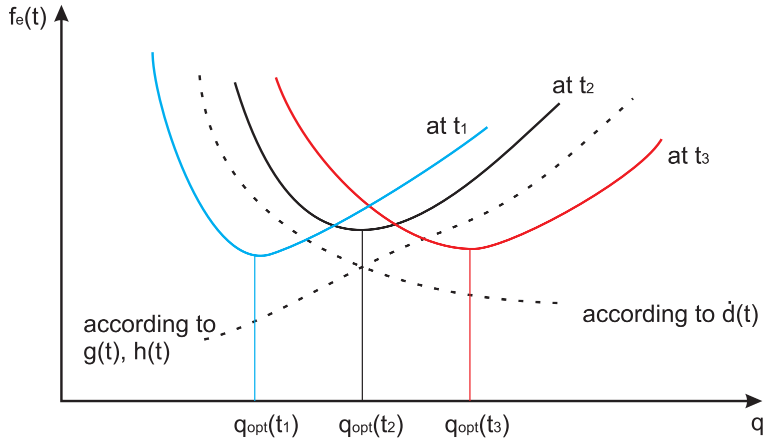

Figure 1: Relations between the estimation error $\boldsymbol{f_e}(t)$ and the design parameter q

where

$$\tilde{\boldsymbol{H}}_1 = \boldsymbol{A}(\boldsymbol{P^a}_{11} - \boldsymbol{P^b}_{11}) + (\boldsymbol{P^a}_{11} - \boldsymbol{P^b}_{11})\boldsymbol{A}^T$$
$$+\boldsymbol{N}(\boldsymbol{P^a}_{12} - \boldsymbol{P^b}_{12})^T + (\boldsymbol{P^a}_{12} - \boldsymbol{P^b}_{12})\boldsymbol{N}^T \geq 0, \quad (27)$$

because $\tilde{\boldsymbol{H}}_1 \in R^{n \times n}$ is one of the principal submatrices of $\tilde{\boldsymbol{H}}$. It follows that

$$\begin{aligned} tr(\tilde{H}_1) &= 2tr(\boldsymbol{A}(\boldsymbol{P^a}_{11} - \boldsymbol{P^b}_{11}) + \boldsymbol{N}(\boldsymbol{P^a}_{12} - \boldsymbol{P^b}_{12})^T) \\ &= \|\boldsymbol{L}_1^a\|_F^2 - \left\|\boldsymbol{L}_1^b\right\|_F^2 \leq 0. \end{aligned} \quad (28)$$

That means $\|\boldsymbol{L}_1^a\|_F \leq \left\|\boldsymbol{L}_1^b\right\|_F$. With the result from i), it holds that

$$\delta^a = \|\boldsymbol{L}_2^a\|_F / \|\boldsymbol{L}_1^a\|_F > \delta^b = \left\|\boldsymbol{L}_2^b\right\|_F / \left\|\boldsymbol{L}_1^b\right\|_F. \quad (29)$$

□

3.1.2. Graphical illustration of the relation between the design parameter q and the estimation error $\boldsymbol{f_e}(t)$

According to Theorem 1., with increasing design parameter q the estimation quality will be improved regarding the increasing ratio δ but be more sensitive to the measurement noise and unmodeled dynamics considering the increasing norm $\|\boldsymbol{L_2}\|_F$. The relations are graphically shown in Fig. 1[3]. At different time point, the minimal level of the estimation error is different. It is obvious that to reach minimum estimation error the design parameter q has to be adjusted online. In the following section, an adaption algorithm is presented.

3.2. Adaption algorithm

Based on the analysis above, an objective function is chosen as

$$\arg\min_{q} \quad J(q), \quad J \;=\; \alpha h {\boldsymbol{e}_{\boldsymbol{y}}}^2(t) + \|\boldsymbol{L}_2\|_F^2 \,, \tag{30}$$

where the parameter α is used for normalization and the variable h denotes the current step size of the numerical time integration of the observer. The measurable estimation error $\boldsymbol{e}_{\boldsymbol{y}}(t) = \boldsymbol{y}(t) - \hat{\boldsymbol{y}}(t)$ in the first part of (30), which is implicitly dependent on the parameter q, represents the estimation error under ideal conditions, namely without measurement noise. On the other hand, the second part of the cost function $J(q)$ is taken into account for the evaluation of effects from unmodeled dynamics and measurement noise. The description of $J(q)$ is to some extent proportional to the estimation quality from the PI-Observer according to the former discussion. The goal here is not to reach the absolute minimal level of the estimation error, but to get acceptable relative minimal levels of the estimation error over the time. Therefore, the search for the local/relative minimal value of the cost function $J(q)$ is a suitable process for adapting the parameter q to get rational relative minimal levels of the estimation error.

A sketch of the adaption process is given in Fig. 2. The adaptive scheme shown in Figure 2 deciding the observer gains to be applied is based on a bank of PI-Observers. The main PI-Observer with the design parameter q_m is the observer which generates the final valid estimation. To realize the rational change, two parallel running PI-Observers which use different design parameters $\alpha = 0.1$ and $\beta = 10$ respectively are included to compare the cost functions J_m, J_l, and J_r for the last step. If the cost function J_m is the smallest one,

[3] Note that the estimation error of the outputs $\boldsymbol{e}_{\boldsymbol{y}}(t)$, of the states $\boldsymbol{e}(t)$, and of the unknown inputs $\boldsymbol{f}_{\boldsymbol{e}}(t)$ are coupled together as mentioned in section 2.

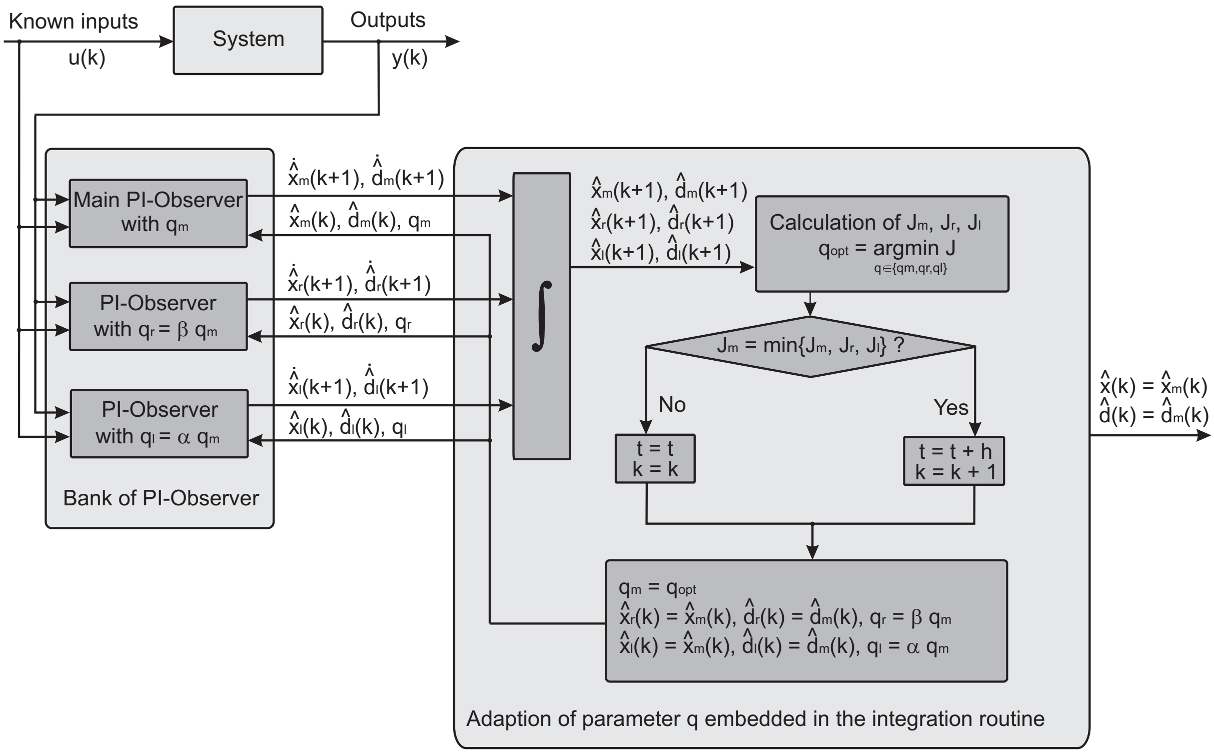

Figure 2: Sketch of proposed adaption process

namely $q_m = q_{opt}$, where $q_{opt} = \arg\min_{q\in\{q_m,q_l,q_r\}} J$, then the estimation results will be taken as valid and the integration will go on.

Otherwise the estimation results will not be taken and the integration will be repeated with new defined $q_m = q_{opt}$, $q_l = 0.1q_m$, and $q_r = 10q_m$. The integration will go on for the next step until it fulfills $q_m = q_{opt}$. The step size h is controlled inside the integral algorithm with the integrated step-size control.

Briefly speaking, the task of the optimization is to keep the design parameter q_m of the main PI-Observer always having the relative minimal value of the cost function.

3.3. Stability of the estimation error dynamics

According to the algorithm illustrated in Fig. 2, the observer gain changes stepsize-wise. In general, the changing observer gains can lead to an unstable estimation error dynamics even if every observer gain matrix is designed to make the error dynamics converge asymptotically.

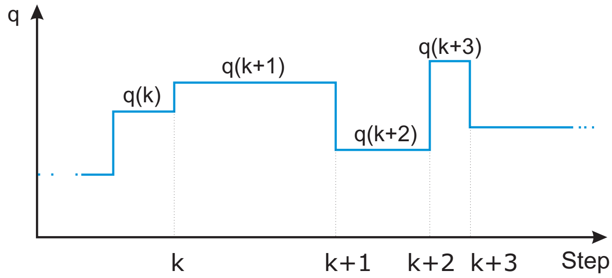

Figure 3: Illustration of the changing gains

The stability condition for switching observers has been already addressed in many literatures, e.g., in [5]:

If all the observer gains are chosen/designed to have the Euclidean norm of the estimation error as a Lyapunov function of the error dynamics, then the estimation error will vanish asymptotically.

For the case which is considered in this paper, the observer matrix $\boldsymbol{L}$ is designed using LQR method for different design parameters q. That indicates that a piecewise Lyapunov function of the estimation error dynamics exists, but it can not ensure the convergence of the estimation error during the changing of observer gains. However, the convergence of the estimation error can be proven, if the condition for the changing is taken into account. The reason is that the observer gain respectively the parameter q is changed only if the cost function J from the current observer gains, which is to some extent proportional to the norm of the estimation error, is no more the local minimal one. That is to say, the change is towards the direction that makes the cost function J smaller, which ensures the convergence of the estimation error.

In order to explain it more clearly, an adaption example of the API-Observer among three parameters q_i, q_{ii}, and q_{iii} is shown in Fig. 4. It is known that if the change of parameter q is arbitrary among the three parameters, the whole trajectory of the cost function J as well as the estimation error of API-Observer may diverge in case that the switch is alway

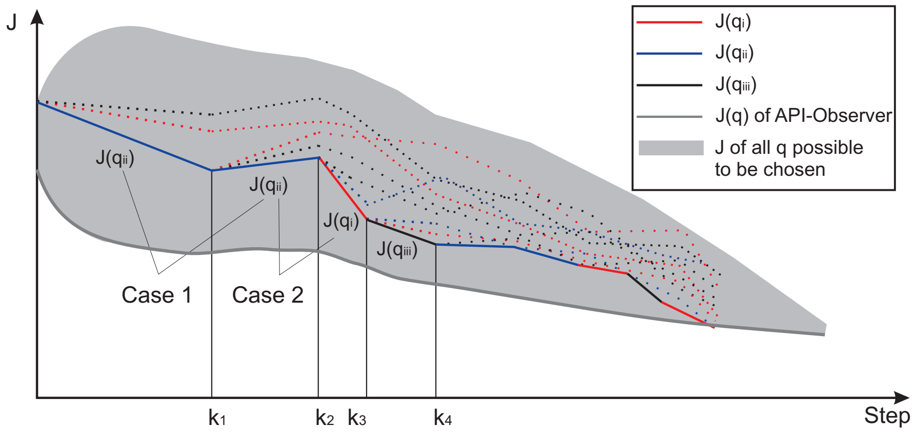

Figure 4: Cases of changing parameter q illustrated by cost function J

towards the direction of a larger J, although the observer design is Hurwitz stable for every parameter. However, in the considered example with the given three parameters the variable parameter q is chosen with the proposed adaptive scheme to keep the cost function J at a minimal level as marked with the colored solid line in Fig. 4. The adaptive parameter q in this example is $q(k_1) = q(k_2) = q_{ii}$, $q(k_3) = q_i$, and $q(k_4) = q_{iii}$. The convergence of the estimation error is discussed as follows. There exist two possible cases for the change of parameter q: the first possibility is the one as shown by Case 1 that the cost function J from one design parameter q_{ii} is the minimal one for two consecutive steps t_1 and t_2, namely $J_{min}(k_1) = J(q_{ii}, k_1)$ and $J_{min}(k_2) = J(q_{ii}, k_2)$; the second case is that the minimal cost function in the last step is no more the minimal one in the following step as shown by Case 2 with $J_{min}(k_2) = J(q_{ii}, k_2)$ and $J_{min}(k_3) = J(q_i, k_3)$. For Case 1, the convergence of the cost function J as well as the estimation error is guaranteed by the asymptotic design with parameter q_{ii}. For Case 2, the estimation error converges towards zero, because the change of parameter q is made to get a smaller cost function $(J(q_i, k_3) < J(q_{ii}, k_3))$ where the speed of convergence is even faster than with the parameter $q(k_3) = q_{ii}$. This discussion can be extended to the general case of API-Observer with uncertain number of parameters q for choosing. Considering the shaded area in Fig. 4 as all possible values of J, the final trajectory of the cost function from an API-Observer with uncertain number of parameters

q for choosing will be the gray solid line that ensures the convergence of the estimation error towards zero.

4. Simulation example

An elastic beam example [8] shown in Fig. 5 is given here to illustrate the proposed approach.

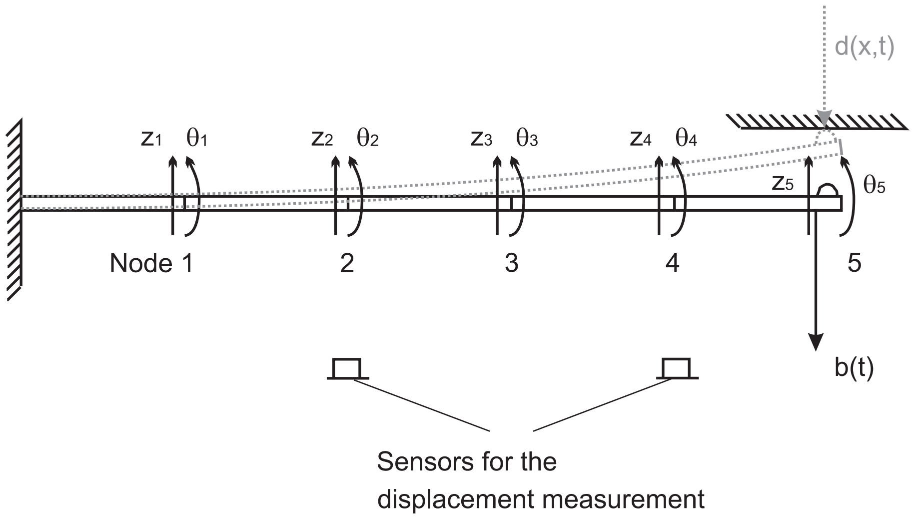

Figure 5: Modeled structure of the beam

The elastic beam system is modeled using Finite Element Method. The length of each element is 98 mm, the cross-sectional area is 125 mm^2. The displacements z_i and the angles θ_i ($i = 1, \cdots, 5$) as well as the corresponding velocities and angular velocities are considered as the system states.

The system model can be described in the standard state space form

$$\dot{\boldsymbol{x}}(t) = \boldsymbol{A}\boldsymbol{x}(t) + \boldsymbol{b}(t) + \boldsymbol{N}d(x,t), \tag{31}$$

$$\boldsymbol{y}(t) = \boldsymbol{C}\boldsymbol{x}(t) + \boldsymbol{C}_h\boldsymbol{h}(t), \tag{32}$$

with the state vector

$$x(t) = \begin{bmatrix} z_1 & \theta_1 & \cdots & z_5 & \theta_5 & \dot{z}_1 & \dot{\theta}_1 & \cdots & \dot{z}_5 & \dot{\theta}_5 \end{bmatrix}^T, \tag{33}$$

one known input $b(t)$, one unknown input $d(x,t)$ acting at the moment of contact between vibrating beam and contact device. Two measurements, the displacements at the third and the fourth nodes ($y_1(t) = x_3(t)$, $y_2(t) = x_7(t)$), are taken. The task is to estimate the unknown and not measured contact force $\boldsymbol{d}(x,t)$ acting on the last node of the beam.

The relevant matrices are the system matrix $\boldsymbol{A} = \begin{bmatrix} \boldsymbol{0}_{10\times 10} & \boldsymbol{I}_{10\times 10} \\ -\boldsymbol{M}^{-1}\boldsymbol{K} & -\boldsymbol{M}^{-1}\boldsymbol{D} \end{bmatrix}$, input matrix $\boldsymbol{N} = \begin{bmatrix} \boldsymbol{0}_{18\times 1} \\ 1 \\ 0 \end{bmatrix}$, the output matrix $\boldsymbol{C} = \begin{bmatrix} \boldsymbol{0}_{1\times 2} & 1 & \boldsymbol{0}_{1\times 17} \\ \boldsymbol{0}_{1\times 6} & 1 & \boldsymbol{0}_{1\times 13} \end{bmatrix}$, and $\boldsymbol{C_h} = \begin{bmatrix} c_{x3} \\ c_{x7} \end{bmatrix}$, where in the simulation it is assumed that $c_{x3} = 0.3$ and $c_{x7} = 1$.

The stiffness matrix $\boldsymbol{K}$ and the mass matrix $\boldsymbol{M}$ are calculated using finite element theory. The damping matrix is taken as $\boldsymbol{D} = \xi\boldsymbol{K}$, where ξ is suitably chosen (using raleigh damping hypothesis).

For the simulation, the contact force calculation is realized by

$$d(x,t) = -3.8 \times 10^6 (x_9(t) - 1 + 5 \times 10^{-4})^2, \tag{34}$$

if the displacement of the last node fulfills $x_9(t) \geq 1$ representing a nonlinear and stiff elastic contact, which is unknown to the observer. It is assumed that white noise $\boldsymbol{h}(t)$ with amplitudes of 0.5% of the measurements is included. Furthermore, certain model uncertainty is taken into account, here the real damping coefficient ξ is 10% larger than the nominal value which is used in the observer.

In Fig. 6 and Fig. 7, the estimations of the unknown input and the displacement at node 5 from the API-Observer are compared with the estimations of two normal PI-Observers with constant design parameters $q = 10^{10}$ and $q = 10^{14}$ respectively. It is clearly shown that with a large constant design parameter $q = 10^{14}$ the estimation of the unknown input is strongly influenced by the measurement noise. In contrast, the estimation from the PI-Observer with low design parameter $q = 10^{10}$ shows almost no effect from the measurement noise and model uncertainty but a large delay time and a non precise amplitude of the estimated contact force. The estimations from the API-Observer combines the advantages of both

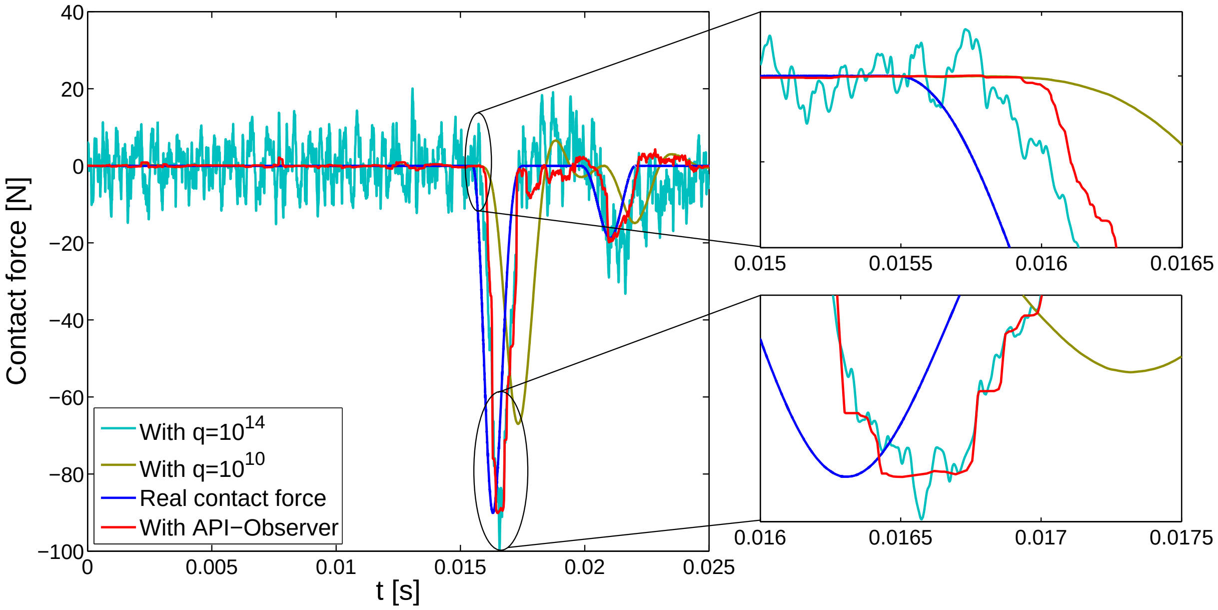

Figure 6: Estimation results of the contact force

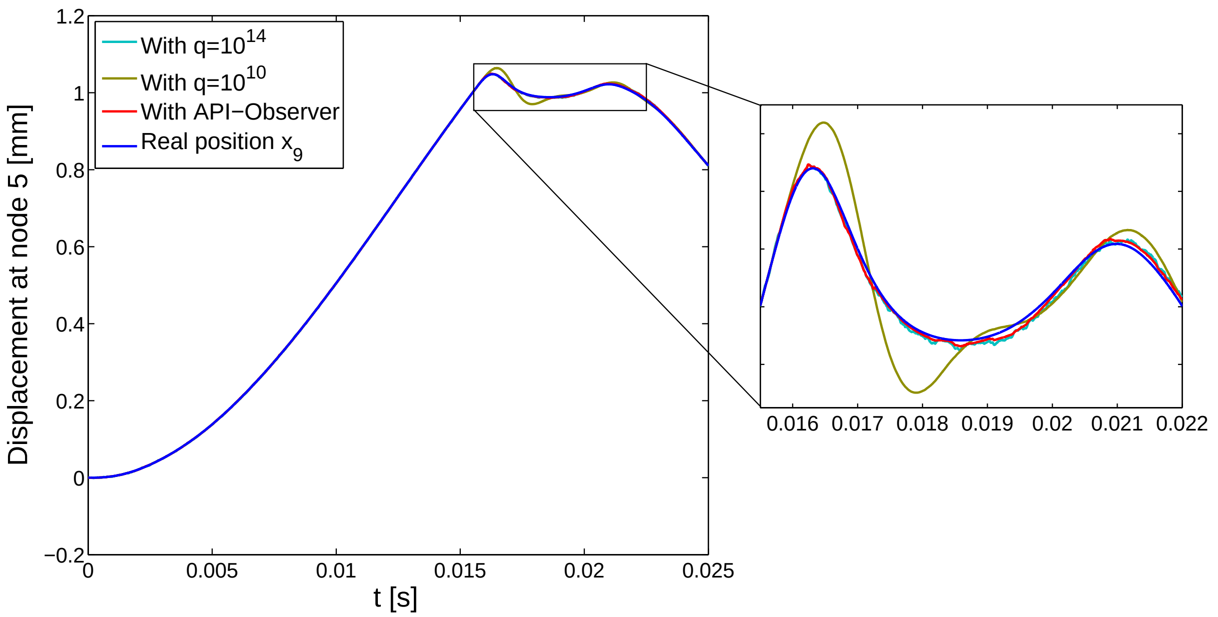

Figure 7: Estimation results of the displacement (at node 5)

the high and low parameters for q. The estimated contact force from the API-Observer reacts rapidly as with a high design parameter q and shows no strong influence from the measurement noise and the unmodeled dynamics. The same results can also be found clearly in the estimation of the displacement x_9.

In Fig. 8, the changing parameter q in the adaption process is given. It can be found that during the time intervals when the contact exists the design parameter q is adjusted to be larger than without contact. That is exactly what the adaptive scheme should realize.

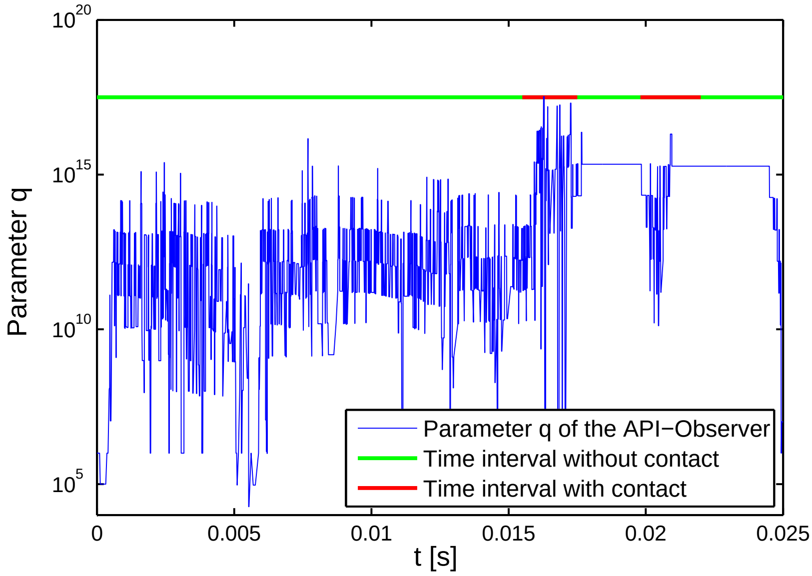

Figure 8: Online adjusted parameter q

As a conclusion, it can be stated, that the online adaption of the PI-Observer design is necessary for estimation improvement and can be realized by the proposed approach as shown.

5. Conclusion

This paper presents the first time an API-Observer design based on online adaption of observer gains integrated in the numerical realization of the observer. A general analysis of the high gain PI-Observer design is given and the stability of the estimation error dynamics is proven. A practical simulation example shows the effects and functionality of the adaption process. From the algorithmic design, it can be concluded that the online variable gain PI-Observer design can attenuate the influence from the measurement noise and unmodeled dynamics significantly. The shown simulation results verify this statement, the results show in detail a very good quality of the unknown inputs estimation. Using this easy-to-realize approach now the API-Observer can be used in more complex task with respect to measurement noise and so on.

References

[1] J. H. Ahrens, H. K. Khalil, High-gain observers in the presence of measurement noise: A switched-gain approach, Automatica 45 (2009) 936–943.

[2] S. Beale, B. Shafai, Robust control system design with a proportional-integral observer, International Journal of Control 50 (1989) 97–111.

[3] E. M. Elbeheiry, H. A. Elmaraghy, Robotic manipulators state observation via one-time gain switching, Journal of Intelligent and Robotic Systems 38 (2003) 313–344.

[4] I. Krajcin, Einsatz des PI-Beobachters zur modellbasierten Diagnose und Regelung elastischer mechanischer Strukturen (Dissertation), Shaker Verlag, Aachen, 2006.

[5] J. Lunze, An example for the design of switching observers, at - Automatisierungstechnik 48 (2000) 556–562.

[6] P. C. Müller, J. Lückel, Zur Theorie der Störgrößenaufschaltung in linearen Mehrgrößenregelsystemen, Regelungstechnik 25 (1977) 54–59.

[7] H. Niemann, J. Stoustrup, B. Shafai, Fault detection using PI observers, in: In Proceedings of Control 97, 1997.

[8] D. Söffker, New results of the development and application of robust observers to elastic mechanical structures, in: H. Ulbrich, W. Günthner (Eds.), Vibration control of nonlinear mechanism and structures, solid mechanics and its applications, Springer 130 (2005) 319–330.

[9] H. K. Wimmer, Monotonicity of maximal solutions of algebraic riccati equations, Systems & Control Letters 5 (1985) 317–319.

[10] B. Wojciechowski, Analysis and synthesis of proportional-integral observers for single-input single-output time-invariant continuos systems, Gliwice, Poland, 1978.

List of Figures

1 Relations between the estimation error $\boldsymbol{f_e}(t)$ and the design parameter q . . 10

2 Sketch of proposed adaption process 12

3 Illustration of the changing gains 13

4 Cases of changing parameter q illustrated by cost function J 14

5 Modeled structure of the beam 15

6 Estimation results of the contact force 17

7 Estimation results of the displacement (at node 5) 17

8 Online adjusted parameter q 18